A MODEL OF ROTATIONALLY-SAMPLED WIND TURBULENCE FOR PREDICTING FATIGUE LOADS IN WIND TURBINES

N95- 27972

David A. Spera

DASCON Engineering
Bay Village, Ohio 44140

ABSTRACT

Empirical equations are presented with which to model rotationally-sampled (R-S) turbulence for input to structural-dynamic computer codes and the calculation of wind turbine fatigue loads. These equations are derived from R-S turbulence data which were measured at the vertical-plane array in Clayton, New Mexico. For validation, the equations are applied to the calculation of cyclic flapwise blade loads for the NASA/DOE Mod-2 2.5-MW experimental HAWTs, and the results compared to measured cyclic loads. Good correlation is achieved, indicating that the R-S turbulence model developed in this study contains the characteristics of the wind which produce many of the fatigue loads sustained by wind turbines. Empirical factors are included which permit the prediction of load levels at specified percentiles of occurrence, which is required for the generation of fatigue load spectra and the prediction of the fatigue lifetime of structures.

INTRODUCTION

The objective of this study is to draw together two phenomena relating to the structural-dynamic response of horizontal-axis wind turbines (HAWTs). The first is the under-prediction of one category of blade loads on the three NASA/DOE Mod-2 experimental HAWTs located near Goldendale, Washington. One of these 3.2-MW 91.4-m diameter turbines is shown in Figure 1. Measured cyclic flapwise bending moments (in and out of the plane of revolution) have been found to be significantly higher than design predictions based on winds measured from a fixed frame of reference [Boeing 1982].

The second phenomenon considered here is that termed "rotationally-sampled turbulence," which is calculated from measurements of instantaneous wind speed from a rotating frame of reference [Verholek 1978, Connell 1981, Kristensen and Frandsen 1982, Connell and George 1983a and 1983b, and George 1984]. These measurements provide data for simulating the wind speed variations actually experienced by a section of a rotating HAWT blade. The spectra of rotationally-sampled wind speeds has been found to be very different from that of atmospheric turbulence measured with a stationary anemometer.

Figure 2 illustrates the basic method of measuring rotationally-sampled (R-S) turbulence [Verholek 1978]. Mounted on a line of instrument towers perpendicular to the prevailing wind, a set of anemometers is arranged in a circular pattern in a vertical plane, with center elevation H and radius R (in this case, 24.4 m and 12.2 m, respectively). This set of towers and anemometers is called a "vertical plane array" or VPA, and represents the path followed by a blade section of an imaginary HAWT rotor. The wind speed at each anemometer is continuously recorded. Samples from each record are then taken sequentially from consecutive anemometers around the circle, with the sampling interval time determined by the rotational speed and the number of anemometers. Interpolations are made between consecutive samples in order to synthesize a continuous record which represents the wind speeds that a blade section would experience in the rotating frame of reference.

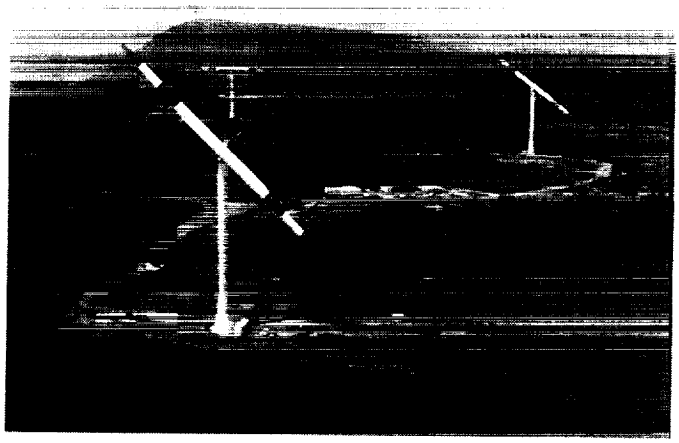

Figure 1. Cluster of three 2.5-MW Mod-2 HAWTs near Goldendale, Washington. (Courtesy of Boeing Aerospace Corporation)

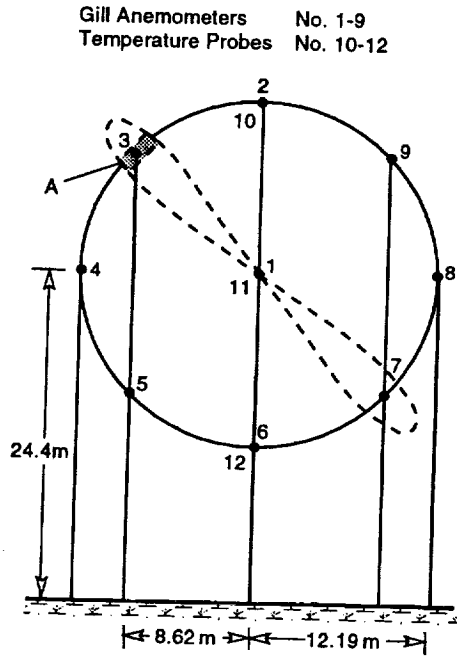

Figure 2. Schematic diagram of a vertical plane array (VPA) of anemometers for measuring wind turbulence experienced by a rotating HAWT blade. Sampling of signals from anemometers 2 to 9 is synchronized with the passage of the hypothetical blade section A. [Verholek 1978]

As illustrated in Figure 3 [Verholek 1978], the power spectrum of rotationally-sampled (R-S) turbulence, line (a), is higher at higher frequencies than that from a stationary anemometer, line (b). Moreover, R-S power is concentrated in "spikes" at frequencies which are integer multiples of the rotational speed. Thus, unsteady wind loading on a rotating HAWT blade may be harmonic in nature, with frequencies equal to multiples of the rotor speed. If so, these wind harmonics could produce a forced harmonic flapwise response in a HAWT blade and increased bending loads.

Drawing together these two phenomena brings us to the purposes of this study, which are (1) to determine if the harmonic content of R-S turbulence is of sufficient size to account for the under-prediction of Mod-2 HAWT cyclic loads, and (2) to develop a practical mathematical model of R-S turbulence that can be used for wind input to structural-dynamic computer codes, resulting in greater accuracy of load predictions.

ROTATIONALLY-SAMPLED TURBULENCE DATA

The R-S turbulence data used in this study were measured by researchers from Battelle's Pacific Northwest Laboratory (PNL) using the VPA located near Clayton, New Mexico [Connell and George 1983a and 1983b, and George and Connell 1984]. The dimensions of this array were H = 30.5 m and R = 19.0 m, and the rotational frequency was 0.667 Hz. Power spectral densities (PSDs) of 8.5-min segments of the synthesized wind speed were created using a Fast Fourier Transform (FFT) technique. Integration of a PSD over a selected frequency band then gave the variance of speed within this band. R-S turbulence in the frequency band is the square-root of this variance. Dividing the turbulence by the steady wind speed at elevation H then gives the R-S turbulence intensity for the selected frequency band.

Table 1 presents typical data reported by PNL researchers for one data segment. A total of 17 data segments form the basis of the R-S turbulence model developed in this study, taken from the following references: 3 from Connell and George [1983a and 1983b], 12 from George and Connell [1984], and 2 from Powell, Connell, and George [1985]. Of these, 10 were for atmospheric stability conditions ranging from neutral to unstable, while 7 were for stable conditions. Stable atmospheres typically result in larger vertical gradients in wind speed and smaller mixing between winds at different elevations. For a discussion of the influence of atmospheric stability on wind shear, see Frost and Aspliden [1994, pp. 392-396].

TABLE 1. TYPICAL CLAYTON VPA WIND DATA
[George and Connell, 1984]

Data Segment Number	= C2c
Date; Starting Time	= 06/30/82; 1740
Test Segment Length	= 8.5 min
Rotational Sampling Speed, P	= 0.67 Hz
Center Mean Wind Speed, U_0	= 10.71 m/s
Center Turbulence, σ_0	= 0.856 m/s
Wind Shear Across Disk, ΔU	= 1.506 m/s

Frequency Band (Hz)	Mid-band Frequency f/P	Variance μ $(m/s)^2$	Turbulence σ (m/s)	Turbulence Intensity σ/U_0
< 0.33		0.498	0.706	0.066
0.33 - 1.00	1	0.431	0.656	0.061
1.00 - 1.67	2	0.146	0.382	0.036
1.67 - 2.33	3	0.070	0.264	0.025
2.33 - 3.00	4	0.037	0.192	0.018
3.00 - 3.67	5	0.032	0.179	0.017

MODEL OF ROTATIONALLY-SAMPLED TURBULENCE

Modeling the Clayton VPA Data

To develop a general model of the Clayton VPA results, turbulence intensities for each harmonic number (*i.e.* mid-band frequency/rotational speed) were plotted *vs* the normalized wind shear measured vertically across the disk, $\Delta U/U_0$, as shown in Figure 4. It can be seen from the trend lines in these plots that (1) only the first harmonic turbulence intensities vary significantly with wind shear across the disk, and its variation is linear, (3) turbulence intensities for each harmonic above the first are roughly equal for all data segments, and (3) atmospheric stability has little, if any, effect on harmonic turbulence intensities.

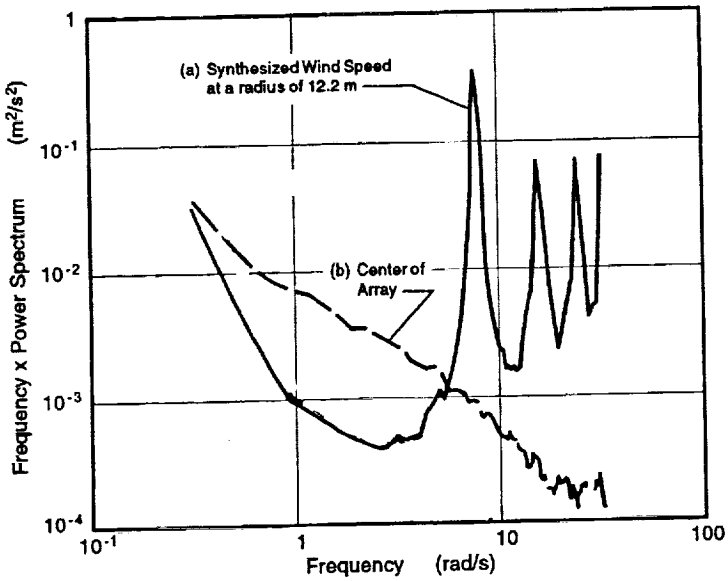

Figure 3. Sample power spectra measured at a VPA, illustrating typical characteristics of both rotationally-sampled and stationary time series of wind speed. (a) Rotationally-sampled wind speeds synthesized into a continuous time series, showing characteristic spikes at multiples of the 7.8 rad/s rotation rate. (b) Stationary time series from the center anemometer in the VPA. [Verholek 1978]

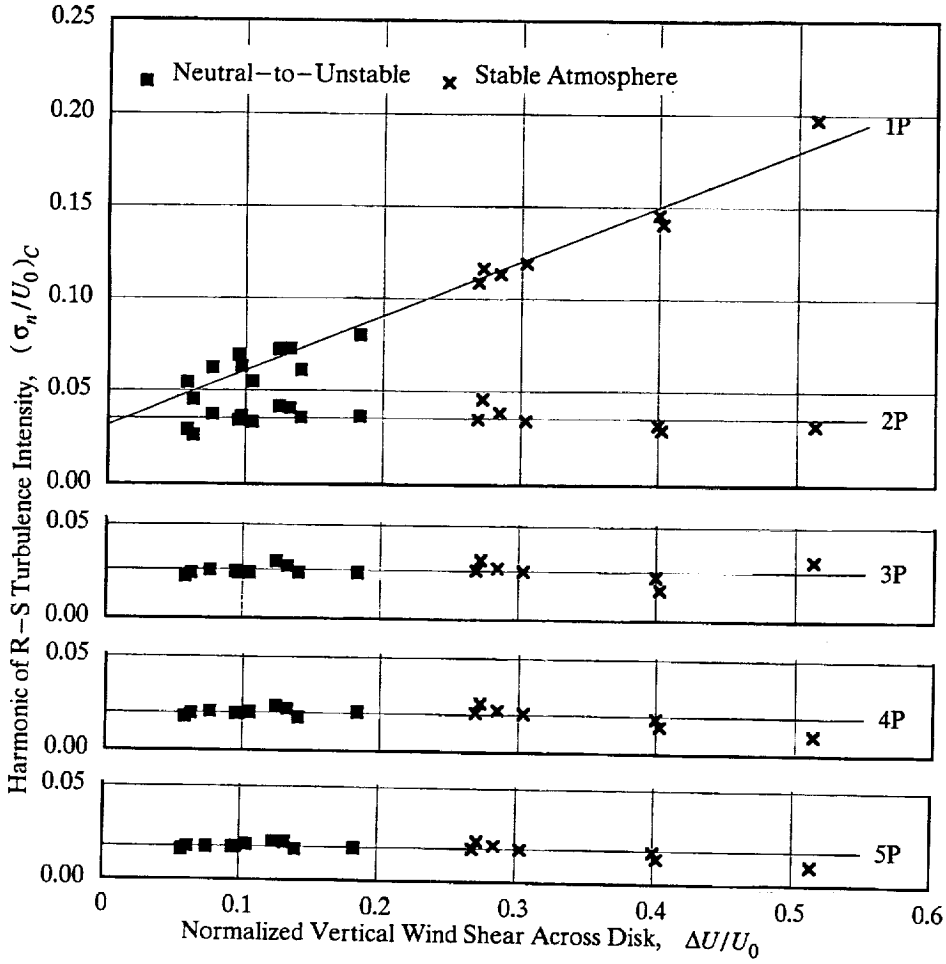

Figure 4. Rotationally-sampled turbulence intensities measured at the Clayton VPA at harmonic frequencies equal to integer multiples of the rotational speed, under neutral-to-stable and unstable atmospheric conditions. Only the first harmonic is influenced by the vertical wind shear across the sampled disk area. [data from PNL]

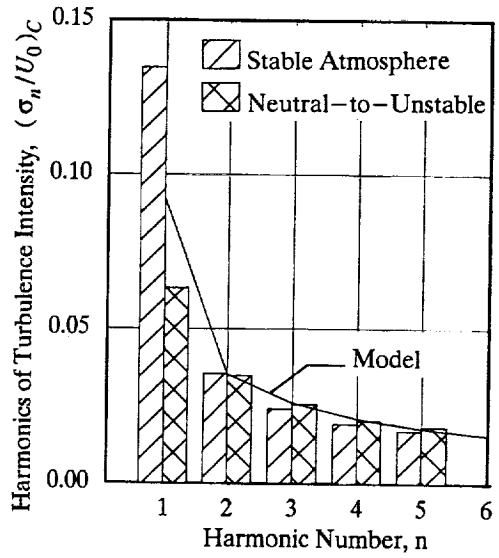

Figure 5. Measured and model harmonic turbulence intensities from the Clayton VPA data. [data from PNL]

Figure 5 presents these same data in another format. Each bar in this figure represents the average turbulence intensity for a given harmonic and atmospheric condition. Again we see that for harmonics above the first, atmospheric stability has little effect. For the first harmonic, the difference between the neutral-to-stable and stable intensities is a result of the larger wind shear across the disk for the stable condition.

The trend line in Figure 5 illustrates the model created here to represent the relationship between R-S turbulence intensity and harmonic number, as defined by the Clayton VPA data. This model is as follows:

$$(\sigma_1/U_0)_C = 0.0311 + 0.297\,\Delta U/U_0 \qquad (1a)$$

$$(\sigma_n/U_0)_C = 0.059\,n^{-0.75} \qquad n > 1 \qquad (1b)$$

where

σ_n = rotationally-sampled turbulence in the frequency range from $(n - 1/2)P$ to $(n + 1/2)P$ (m/s)
P = rotational sampling frequency (rad/s)
C = subscript denoting Clayton VPA parameters
U_0 = steady free-stream wind speed at hub elevation (m/s)
ΔU = total steady wind shear from top to bottom of rotor swept area (m/s)

We can calculate the steady wind shear across the disk, ΔU, from the well-known logarithmic/linear model of the vertical gradient in the steady wind speed, which is as follows [Frost and Aspliden 1994, pp. 392-395]:

$$U = U_0 \frac{\ln(z/z_0) + \Psi_S(z/L_S)}{\ln(H/z_0) + \Psi_S(H/L_S)} \quad (2)$$

where

z = elevation above ground level (m)
z_0 = surface roughness length (m)
H = elevation of hub above ground (m)
R = tip radius of rotor (m)
Ψ_S = atmospheric stability function dependent on z/L_S
$\langle\ \rangle$ = function of $\langle\ \rangle$
L_S = Monin-Obukhov stability length (m)

For the purposes of this study, we will assume neutral atmospheric stability, for which the function Ψ_S is equal to zero. As shown in Figure 5, this results in a model prediction of the first harmonic turbulence that is intermediate between measurements made under stable and neutral-to-unstable atmospheric conditions. The first harmonic is not a critical wind loading on a teetered-hub rotor like that of the Mod-2 HAWT. For a fixed-hub rotor, however, the first harmonic can be important and the assumption of a stable atmosphere may be reasonable. With the assumption of neutral atmospheric stability, Equation (2) leads to the following expression for the wind shear vertically across a circle of radius R with its center at elevation H:

$$\Delta U/U_0 = \frac{\ln[(H+R)/(H-R)]}{\ln(H/z_0)} \quad (3)$$

Scaling Clayton VPA Data to Other Radii and Elevations

To generalize Equations 1, we must now make additional assumptions about the effects of R and H on R-S turbulence intensity. First, we will assume that the R-S sampling path length and the period for one revolution both increase linearly with sampling radius, which is compatible with general practice of operating HAWT blades at approximately the same tip speed independently of rotor diameter. The longer sampling paths and sampling periods of larger rotors are assumed to result in larger wind speed variations around the perimeter of the sampled circle. For simplicity, this relationship between increasing sampling radius and increasing R-S turbulence intensity is assumed to be linear.

The effect of center elevation on R-S turbulence is assumed to be approximately the same as the elevation effect on turbulence measured at a fixed point. According to Frost and Aspliden [1994, p. 407], an acceptable model for the effect of elevation on longitudinal turbulence at a fixed point is

$$\frac{\sigma_{0,x}}{U_0} = \frac{0.52}{\ln(H/z_0)\,(0.177 + 0.00139\,H)^{0.4}} \quad (4)$$

where $\sigma_{0,x}$ = longitudinal turbulence at a fixed point (m/s)

Combining a linear effect of sampling radius with the effect of center elevation given in Equation 4, we obtain

$$\frac{\sigma_n/U_0}{(\sigma_n/U_0)_C} = \frac{R}{R_C} \frac{[\ln(H/z_0)\,(0.177 + 0.00139\,H)^{0.4}]_C}{\ln(H/z_0)\,(0.177 + 0.00139\,H)^{0.4}} \quad (5a)$$

Once again, the subscript C denotes parameters of the Clayton VPA, which are R_C = 19.0 m, H_C = 30.5 m, and $z_{0,C}$ = 0.024 m. After substituting these Clayton parameters into Equation (5a), the following scaling equation is derived for the R-S turbulence intensities along the tip path of a general HAWT rotor:

$$\frac{\sigma_n}{U_0} = \frac{0.204\,R}{\ln(H/z_0)\,(0.177 + 0.00138\,H)^{0.4}} \left(\frac{\sigma_n}{U_0}\right)_C \quad (5b)$$

where the Clayton intensities $(\sigma/U_0)_C$ are given by Equations (1).

Spatial Distribution Around the Sampling Circle

The next step in the development of this R-S turbulence model is defining a time-history of wind speed around the sampling circle, in a format that can be used as input to structural-dynamic computer codes. The R-S turbulence is assumed to be quasi-static, which means that a HAWT rotor makes several revolutions before any significant changes occur in the spatial distribution of the wind within the rotor's swept area. Dynamic responses of the rotor blades are assumed to approach a steady state before the wind turbulence changes. With this quasi-static assumption, the time-varying unsteady wind can be converted to a spatially-varying steady wind, for which we shall use the following harmonic format:

$$U_{RS} = U_0 + \Sigma\,(A_n \cos n\psi) \quad n = 1, 2, \ldots \quad (6)$$

where

U_{RS} = rotationally-sampled free-stream horizontal wind speed, quasi-steady in time (m/s)
A_n = amplitude of nth harmonic of wind speed (m/s)
ψ = azimuthal position in rotor disk area; 0 = down (deg)

Wind turbulence is equal to the standard deviation of the wind speed from its steady value. For each cosine wave in Equation (6), standard deviation and amplitude are related as follows:

$$|A_n| = \sqrt{2}\ \sigma_n \quad (7)$$

While the absolute values of the harmonic amplitudes can be determined from R-S turbulence data, the signs of these amplitudes cannot. Various patterns of positive and negative signs (equivalent to in-phase and out-of-phase harmonics in Eq. (6)) have been used. For example, Zimmerman *et al.* [1995] assumed negative amplitudes for odd-numbered harmonics and positive amplitudes for even-numbered harmonics. Here we shall obtain a pattern of amplitude signs by examining the resulting vertical wind profile for reasonableness.

Figure 6 [Frost and Aspliden 1994, pg. 391] illustrates the general shapes of typical vertical profiles of the wind speed. To be reasonable, the fluctuations in the quasi-steady profile of our R-S turbulence model should be intermediate between those of the "instantaneous" and "steady" profiles in this figure. Of the many possible combinations of positive and negative harmonic amplitudes, the most reasonable vertical profile is obtained with negative harmonics except for the third and fourth, as shown in Figure 7. The vertical profile obtained with this combination is shown in Figure 8 for the Clayton VPA. Figure 9 illustrates the same spatial distribution of quasi-steady wind speed, but this time as seen by a blade section moving around the sampling circle of the Clayton VPA.

Spatial Distribution Along a HAWT Blade

The final step in the development of an R-S turbulence model of the quasi-steady wind speed within the swept area of a HAWT rotor is defining the wind speed distribution from hub to tip. Earlier the assumption was made that size of R-S turbulence harmonics varied linearly with the sampling radius. However, this assumption alone is not sufficient to define the simultaneous wind

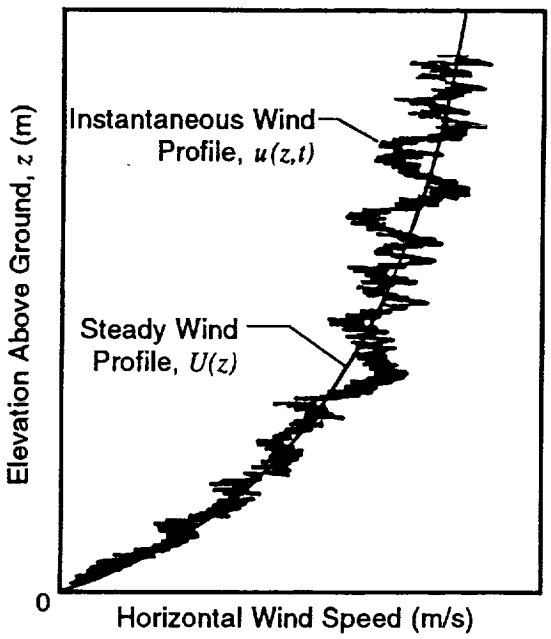

Figure 6. Typical vertical profiles of the wind speed, both instantaneous and steady. [Frost and Aspliden 1994]

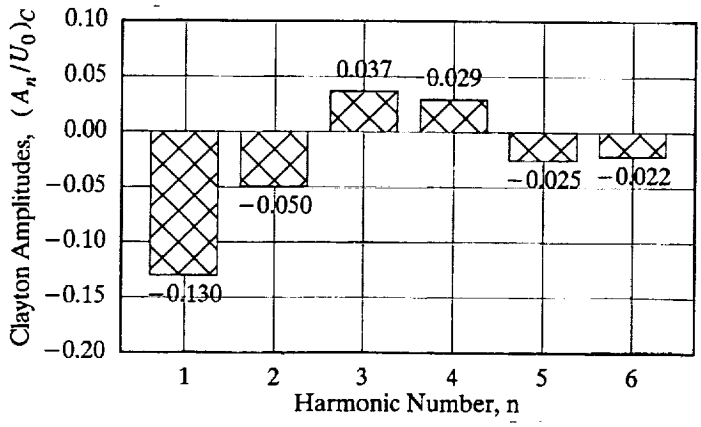

Figure 7. Proposed model amplitudes of rotationally-sampled wind speed for the parameters of the Clayton VPA: R = 19.0 m, H = 30.5 m, and z_0 = 0.024 m. Positive and negative signs are selected to obtain vertical profiles similar to those in Figure 6.

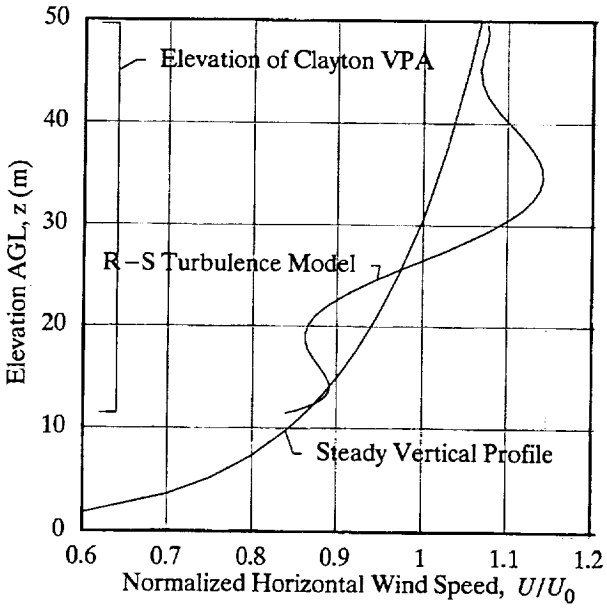

Figure 8. Vertical profile of the wind speed around the Clayton VPA sampling circle, as given by the proposed R-S turbulence model.

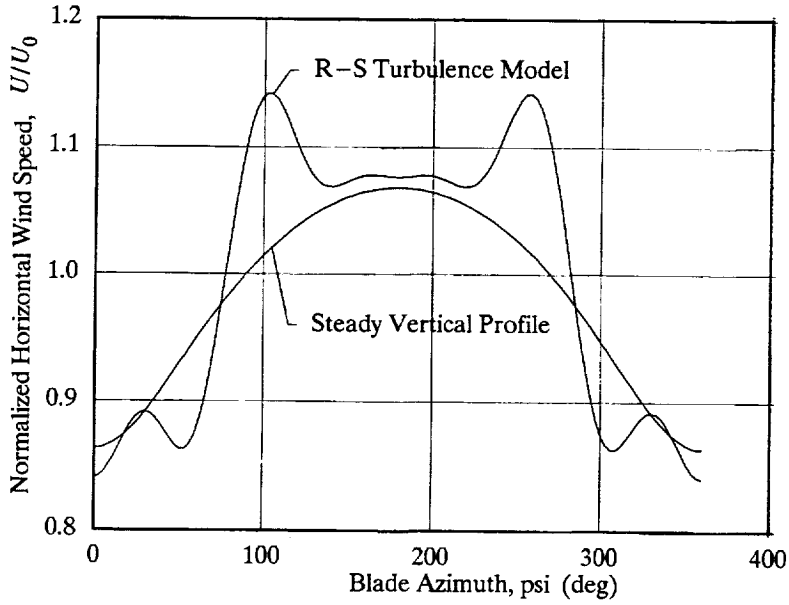

Figure 9. Spatial distribution of the wind speed around the Clayton VPA sampling circle, as given by the proposed R-S turbulence model.

speeds at radii smaller than the sampling radius, because the spanwise distribution of turbulence also depends strongly on the transverse coherence of the wind [Frost and Aspliden, 1994, pg. 410-411, 418]. Coherence is a dimensionless quantity between zero and unity that represents the degree to which two unsteady events, separated in space, are alike in their time histories. If the two time histories are identical their coherence is unity, and if they are completely unrelated their coherence is zero.

Coherences of individual harmonics of R-S turbulence were measured by Zimmerman *et al.* [1995] using wind speed sensors mounted at two locations 69.2 ft apart on a 150-ft Mod-2 HAWT blade. These data are shown in Figure 10, in which the outboard location (r = 100 ft) is taken as the reference and therefore has, by definition, a coherence of 1.00. The coherence between the first harmonic at the inboard location (r = 30.8 ft) and the first harmonic at the outboard station was found to be high, but equivalent coherences of the higher harmonics were all low for this separation distance.

To generalize these observations, trend curves are first drawn to bound the data, following the form

$$coh = \exp\left[-(\zeta/Z)^2\right] \tag{8}$$

where

coh = coherence relative to same harmonic at r_o
r_o = radial distance to reference station (ft)
ζ = separation distance from reference station, $r_o - r$ (ft)
Z = empirical length scale (ft)

These data trends are now idealized for purposes of incorporating coherence into the R-S turbulence model. First, the coherence for the first harmonic is assumed to be 1.00 for all separation distances, because it closely follows the steady vertical profile illustrated in Figure 9.

For the higher harmonics, where coherence decreases with increasing separation distance, a coherence of 0.5 is selected as identifying a transition between unrelated and related time histories. From the trend lines in Figure 10, this transition coherence occurs at an average separation distance of about 42 ft (*i.e.*, r = 38 ft). Following Counihan's empirical model for the integral length scales of crosswind turbulence [Frost and Aspliden 1994, pg. 418], we will assume that the empirical length scale, Z, and the transition separation are both proportional to elevation above ground. Using the Mod-2 tower height of 200 ft as an average elevation, the transition separation distance of 42 ft, obtained from the test data, is generalized to be equal to 0.21 H.

With the idealized model of coherence shown in Figure 10, the spatial distribution of wind harmonic amplitudes along a HAWT blade are given by the following equations in this R-S turbulence model:

$$A_1\langle r\rangle = \frac{r}{R} A_1\langle R\rangle \tag{9a}$$

For $n > 1$: (9b)

$$A_n\langle r\rangle = \frac{r}{R} A_n\langle R\rangle \quad \text{if } (R - r) \le 0.21\,H \tag{9c}$$

$$= 0 \quad \text{if } (R - r) > 0.21\,H$$

where $\langle\,\rangle$ = function of $\langle\,\rangle$

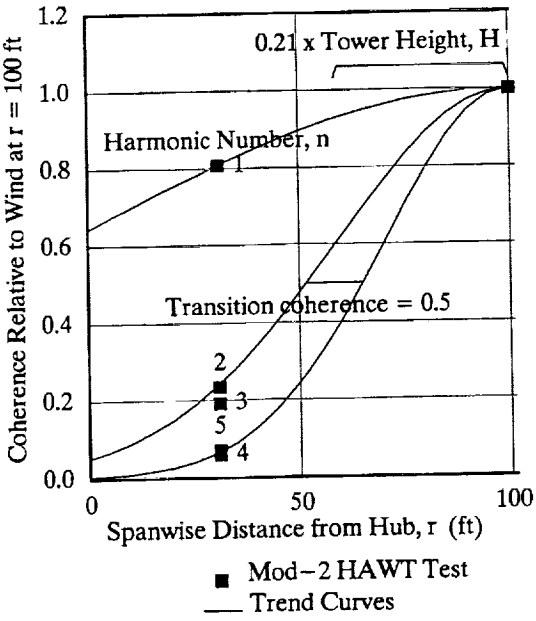

Figure 10. Coherence of individual harmonics of wind speeds rotationally-sampled at two spanwise locations along Mod-2 HAWT blades. [data from Zimmerman *et al.* 1995]

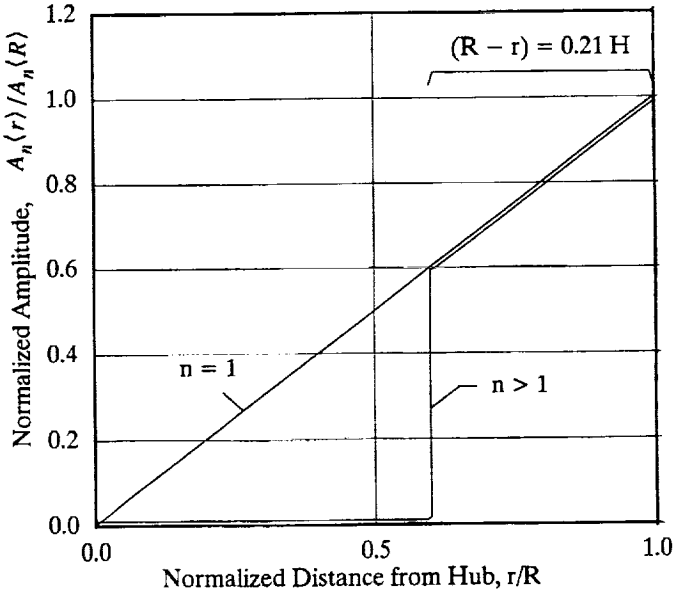

Figure 11. Proposed model of spanwise distribution of harmonic amplitudes of rotationally-sampled turbulence, accounting for reduced coherence of higher harmonics with distance inboard from blade tip.

SUMMARY OF EQUATIONS DEFINING PROPOSED MODEL OF A ROTATIONALLY-SAMPLED TURBULENT WIND FIELD

$$U_{RS}\langle r,R,H,z_0,\psi\rangle = U_0\langle H,z_0\rangle + \text{(10a)}$$

$$+ \frac{r}{R}\sum A_{R,n}\langle R,H,z_0\rangle \cos n\psi \quad n = 1,2,\ldots$$

$$U_0 = U_r\left[\ln(H/z_0)/\ln(z_r/z_0)\right] \quad \text{(10b)}$$

$$A_{R,1} = -U_0\left\{0.04398\,S\langle R,H,z_0\rangle + \right.$$

$$\left. + 0.4120\ln[(H+R)/(H-R)]/\ln(H/z_0)\right\} \quad \text{(10c)}$$

$$S = \frac{0.204\,R}{\ln(H/z_0)(0.177 + 0.00138\,H)^{0.4}} \quad \text{(10d)}$$

If $(R - r) \le 0.21\,H$:

$$A_{R,2} = -0.0496\,S\,U_0 \quad \text{(10e)}$$

$$A_{R,3} = +0.0366\,S\,U_0 \quad \text{(10f)}$$

$$A_{R,4} = +0.0295\,S\,U_0 \quad \text{(10g)}$$

$$A_{R,5} = -0.0250\,S\,U_0 \quad \text{(10h)}$$

$$A_{R,6} = -0.0218\,S\,U_0 \quad \text{(10i)}$$

If $(R - r) > 0.21\,H$:

$$A_{R,n} = 0 \qquad n > 1 \quad \text{(10j)}$$

where

U_{RS} = rotationally-sampled free-stream horizontal wind speed, quasi-steady in time (m/s)
$\langle\ \rangle$ = function of $\langle\ \rangle$
r = radial distance from rotor axis (m)
R = tip radius of rotor (m)
H = elevation of hub above ground (m)
z_0 = surface roughness length (m)
ψ = azimuthal position in rotor disk area; 0 = down (deg)
U_0 = steady free-stream wind speed at hub elevation (m/s)
$A_{R,n}$ = amplitude of nth harmonic of wind speed distribution around circle of radius R (m/s)
U_R = steady free-stream wind speed at reference elevation (m/s)
z_R = reference elevation = 10 m
S = scale factor

APPLICATION TO MOD-2 HAWT FATIGUE LOADS

Discrepancies Between Measured and Design Loads

Figure 12 illustrates the discrepancies that were observed during testing of the Mod-2 HAWTs between measured and design cyclic flatwise blade loads. In this figure, bending loads are plotted as a function of steady free-stream wind speed. The areas marked *C* are envelopes of 50th-percentile loads (*i.e.*, median loads) measured at 21 and 65 percent of span.

The lines marked *A* are load calculations made with the MOSTAB-HFW computer model with a power-law wind shear providing the non-uniform wind field. MOSTAB-HFW is representative of several available codes which contain teetering, flatwise, and chordwise degrees of freedom. Scale model tests in a wind tunnel indicated that cyclic flatwise blade loads were approximately 65% larger than those predicted by this computer model [Boeing 1979]. Therefore, a factor of 1.65 was applied to the computer predictions to produce the design bending loads marked *B* in the figure.

A comparison of the design load lines in Figure 12 with the envelopes of the measured loads clearly shows a significant underprediction of cyclic flatwise bending at both outboard and inboard sections of the blades. Our purpose now will be to apply the rotationally-sampled turbulent wind model just developed in place of the power-law wind shear model used in the Mod-2 design, and eliminate discrepancies between measured and predicted cyclic flatwise bending loads.

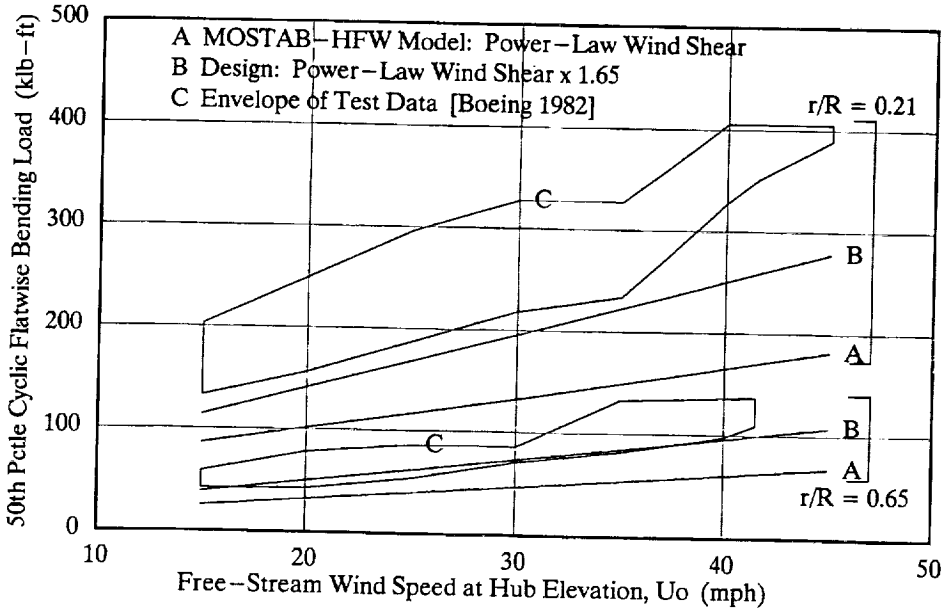

Figure 12. Comparison of calculated and measured cyclic flatwise bending loads at two spanwise locations on a Mod-2 HAWT blade, showing underprediction of design loads at the 50th percentile level. [data from Boeing 1982]

Spectrum Load Factor

The spectrum of fatigue loads experienced by an operating wind turbine is quite wide, even at a given steady wind speed [Spera 1994]. Since the rotationally-sampled turbulence model defined by Equations 10 specifies a single spatial distribution for a specified steady wind speed, we will introduce an empirical load factor to be evaluated later from measured spectra of Mod-2 loads, as follows:

$$\delta L(U_0,p) = \delta L_b(U_0) \times \beta(p) \qquad (11)$$

where

δL = cyclic load = $(L_{max} - L_{min})/2$ during one rotor revolution
p = percentile of load spectrum
δL_b = baseline cyclic load calculated for free-stream wind speed U_0 and non-uniform wind field defined by Equations (10)
β = empirical load factor; function of percentile p

Amplitudes of R-S Wind Model Harmonics

Equations (10) will now be used to define a non-uniform wind field which will be used as an input to a structural-dynamic model of the Mod-2 HAWT rotor, in order to calculate cyclic flatwise bending loads on the rotor blades. Parameters defining the Mod-2 rotor and the roughness of the Goldendale, Washington, site are R = 45.7 m, H = 61.0 m, and z_0 = 0.024 m. With Equations (10) and these dimensions, we can calculate the amplitudes of the various wind harmonics flowing into the structural-dynamic model of the Mod-2 rotor, with the results listed in Table 2.

TABLE 2.
AMPLITUDES OF R-S TURBULENCE HARMONICS
FOR A MOD-2 HAWT AT GOLDENDALE, WASHINGTON

Harmonic Number n	Amplitude Intensity $A_{R,n}/U_o$
1	-0.2653
2	-0.1012
3	+0.0746
4	+0.0602
5	-0.0509
6	-0.0444

RESULTS AND DISCUSSION

Cyclic flatwise bending loads on a Mod-2 rotor blade were calculated using the MOSTAB-HFW code with the proposed R-S turbulence wind model, for two blade stations (r/R = 0.21 and 0.65) and two percentiles (50th and 99.9th). The results are shown by lines D and E in Figures 13 and 14. Load outputs of the MOSTAB-HFW code have been multiplied by values of the factor β selected to produce correlation with average measured loads.

As noted on Figure 13, load factors of 1.00 produce good agreement between 50th percentile calculated and measured loads at both inboard and outboard blade stations. This indicates that the R-S turbulence measured at Clayton, scaled up to the Mod-2 rotor size in Table 2, is sufficient to account for the discrepancies observed between design and measured cyclic loads at the 50th percentile level, without resorting to any other load factors.

In Figure 14, values of β equal to 2.95 and 3.05 were required to scale the MOSTAB-HFW output (again, with the amplitudes in Table 2 as wind input) to the 99.9th percentile load levels at the two blade stations.

In Figure 15, the values of the load factor β which produce agreement between calculated and measured cyclic flatwise bending loads are plotted *vs* the percentile of load, p, on a scale which defines a normal probability distribution. The selection of power-law for the trend curve is based on the log-normal distribution observed for a large quantity of field test data [Spera *et al.* 1984], and is given by the following equation:

$$\beta = 1.00\,(m\,\sigma)^{0.155} \qquad (12)$$

where

σ = standard deviation of load from mean (50th percentile)
m = number of standard deviations for load percentile desired; for example
m = 0 for 50th percentile
m = 1.28 for 90th percentile
m = 2.33 for 99th percentile
m = 3.08 for 99.9th percentile

Thus, once the 50th percentile cyclic flatwise bending loads have been calculated using a structural-dynamics code like MOSTAB-HFW and a wind input defined by Equations (10), a complete spectrum of cyclic loads and resulting fatigue stresses can be calculated by applying Equations (11) and (12). With a cumulative fatigue damage algorithm blade fatigue life can then be estimated [Spera 1994].

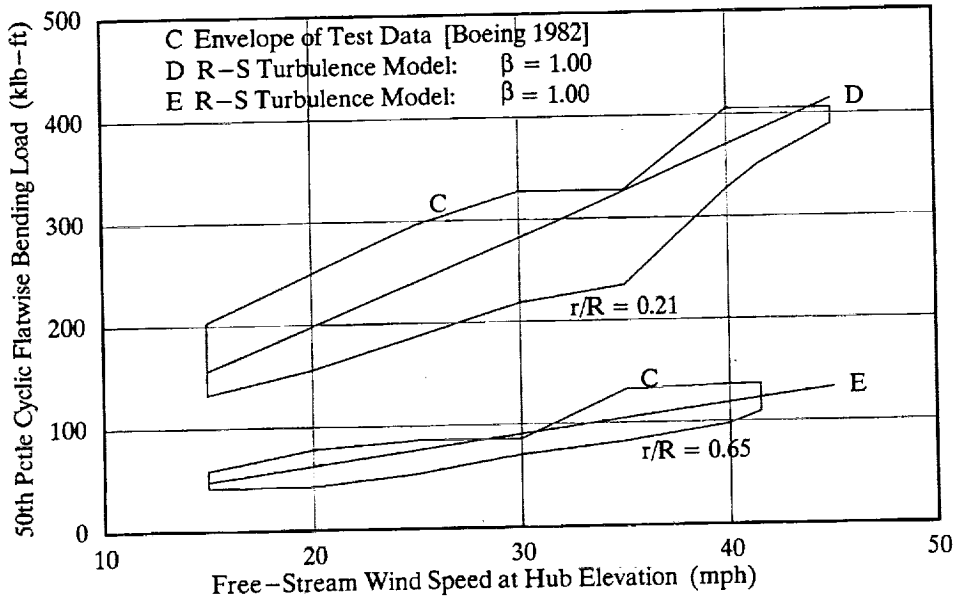

Figure 13. Comparison of 50th percentile cyclic flatwise bending loads calculated using the proposed R-S turbulence model with measured loads. A load factor of 1.00 applied to the output of the MOSTAB-HFW structural-dynamics code is sufficient to obtain correlation both inboard and outboard along the blade. [data from Boeing 1982]

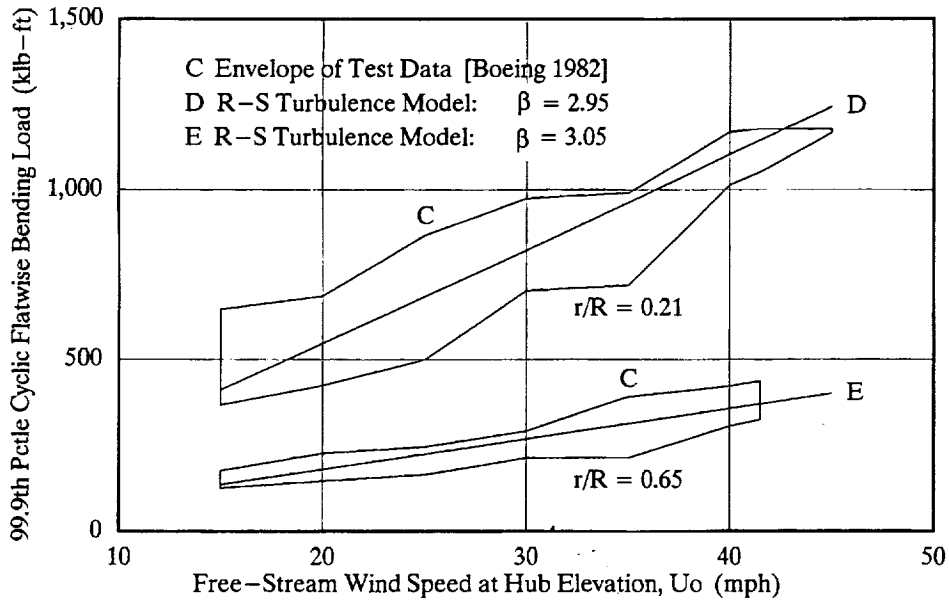

Figure 14. Comparison of 99.9th percentile cyclic flatwise bending loads calculated using the proposed R-S turbulence model with measured loads. Load factors of approximately 3.0 produce correlation both inboard and outboard along the blade. [data from Boeing 1982]

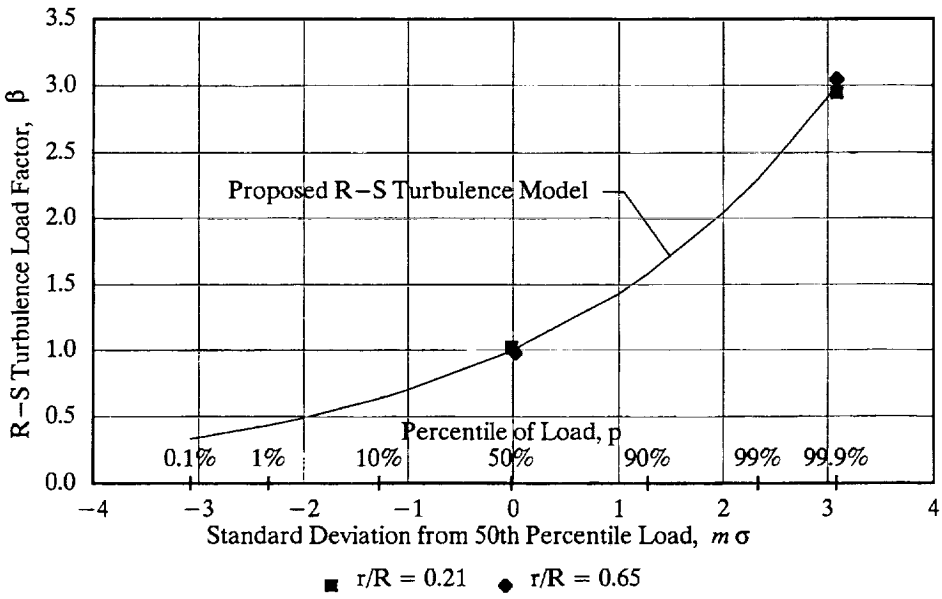

Figure 15. Proposed model of the R-S turbulence load factor with which the spectrum of cyclic flatwise bending loads on a HAWT blade can be calculated from the 50th percentile level of load. The model is based on a log-normal probability distribution.

CONCLUSIONS

1. Rotational sampling of the wind field entering the swept area of a HAWT rotor has shown that turbulence acts as a series of quasi-static harmonic forcing functions on the rotor blades, and that these forcing functions act at frequencies which are integer multiples of the rotor speed.

2. Structural-dynamic computer models of HAWT systems should include R-S turbulence in their wind input modules to adequately evaluate the dynamic response of rotor blades to these harmonic forcing functions and the significance of resulting fatigue damage.

3. Equations are derived herein which define a practical model of a wind field containing R-S turbulence for HAWT structural-dynamic analysis. These equations, based on rotationally-sampled turbulence measured by PNL personnel at the Clayton vertical-plane-array, are in a general form which permits scaling to different rotor diameters, tower elevations, and surface roughnesses.

4. The R-S turbulence measured at the Clayton VPA, scaled up to the Mod-2 HAWT rotor size, is sufficient to account for the discrepancies observed previously between Mod-2 design and measured cyclic loads at the 50th percentile level, without resorting to any other load factors.

5. An empirical load factor model is derived with which the spectrum of cyclic flatwise bending loads on a HAWT rotor blade can be calculated from the 50th percentile load level, based on a log-normal probability distribution typical of many HAWT load spectra.

6. The first harmonic of R-S turbulence intensity is proportional to the steady vertical wind shear across the rotor disk area, but all other harmonics are insensitive to vertical wind shear.

7. Harmonics of R-S turbulence intensity above the first are roughly constant for all wind test conditions.

8. Atmospheric stability has little, if any, effect on harmonic turbulence intensities other than tending to increase the steady vertical wind shear across the rotor disk area and thereby the first harmonic of R-S turbulence.

ACKNOWLEGMENT

David C. Janetzke of the NASA Lewis Research Center performed the MOSTAB-HFW structural-dynamic analysis of the Mod-2 HAWT, adapting the code's wind input module to accommodate the R-S turbulence model. This work was critical to the study, and the author expresses his appreciation.

REFERENCES

Boeing Engineering and Construction, 1982a, "Mod-2 Wind Turbine System Concept and Preliminary Design Report, Volume II: Detailed Report, NASA CR-159609, DOE/NASA 0002-80/2, Cleveland, Ohio: NASA Lewis Research Center, p. 5-2.

Boeing Engineering and Construction, 1982b, "Mod-2 Wind Turbine System Development Final Report, Volume II: Detailed Report, NASA CR-168007, DOE/NASA/0002-2, Cleveland, Ohio: NASA Lewis Research Center, pp. 5-9 to 5-11.

Connell, J. R., 1981, "The Spectrum of Wind Speed Fluctuations Encountered by a Rotating Blade of a Wind Energy Conversion System: Observations and Theory," PNL-4083, Richland, Washington: Battelle Pacific Northwest Laboratory.

Connell, J. R., and George, R. L., 1983a, "A New Look at Turbulence Experienced by a Rotating Wind Turbine," Proceedings, Second ASME Wind Energy Symposium, PNL SA-10653, Richland, Washington: Battelle Pacific Northwest Laboratory.

Connell, J. R., and George, R. L., 1983b, "Scaling Wind Characteristics for Designing Small and Large Wind Turbines," Proceedings, Sixth Biennial Wind Energy Conference and Workshop, B. H. Glenn, ed., Boulder, Colorado: American Solar Energy Society, pp. 513-524.

Frost, W., and Aspliden, C., 1994, "Characteristics of the Wind," in Wind Turbine Technology, D. A. Spera, ed., ASME Press, New York: American Society of Mechanical Engineers, pp. 371-446.

George, R. L., 1984, "Simulation of Winds As Seen by a Rotating Vertical Axis Wind Turbine Blade," PNL-4914, Richland, Washington: Battelle Pacific Northwest Laboratory.

George, R. L., and Connell, J. R., 1984, "Rotationally Sampled Wind Characteristics and Correlations with Mod-0A Wind Turbine Response," PNL-5238, Richland, Washington: Battelle Pacific Northwest Laboratory.

Kristensen, L., and Frandsen, S., 1982, "Model for Power Spectra of the Blade of a Wind turbine Measured from the Moving Frame of Reference," Journal of Wind Engineering and Industrial Aerodynamics, Vol. 10, Amsterdam: Elsevier Scientific Publishing Company, pp. 249-262.

Powell, D. C., Connell, J. R., and George, R. L., 1985, "Verification of Theoretically Computed Spectra for a Point Rotating in a Vertical Plane," PNL-5440, Richland, Washington: Battelle Pacific Northwest Laboratory.

Spera, D. A., Ensworth, C. B. III, and Janetzke, D. C., 1984, "Dynamic Loads in Horizontal-Axis Wind Turbines, Part I: Field Test Data," Proceedings, Wind Power '85 Conference, SERI/CP -217-2902, Golden, Colorado: National Renewable Energy Laboratory, pp. 457-462.

Spera, D. A., 1994, "Fatigue Design of Wind Turbines," in Wind Turbine Technology, D. A. Spera, ed., ASME Press, New York: American Society of Mechanical Engineers, pp. 547-588.

Verholek, M. G., 1978, "Preliminary Results of a Field Experiment to Characterize Wind Flow Through A Vertical Plane," PNL 2518, Richland, Washington: Battelle Pacific Northwest Laboratory.

Zimmerman, D. K., Shipley, S. A., and Miller, R. D., 1995, "Comparison of Measured and Calculated Dynamic Loads for the Mod-2 2.5 MW Wind Turbine System, in Collected Papers on Wind Turbine Technology, D. A. Spera, Ed., NASA CR-195432, DOE/NASA/5776-1, Cleveland, Ohio: NASA Lewis Research Center.